Surface superconductivity as the primary cause of broadening of superconducting transition in Nb films at high magnetic fields

A. Zeinali, T. Golod, and V. M. Krasnov*

Department of Physics, Stockholm University, AlbaNova University Center, SE-10691 Stockholm, Sweden

(Received 2 September 2016; revised manuscript received 26 October 2016; published 12 December 2016)

We study the origin of broadening of superconducting transition in sputtered Nb films at high magnetic fields. From simultaneous tunneling and transport measurements we conclude that the upper critical field H_{c2} always corresponds to the bottom of transition $R \sim 0$, while the top $R \sim R_n$ occurs close to the critical field for destruction of surface superconductivity $H_{c3} \simeq 1.7H_{c2}$. The two-dimensional nature of superconductivity at $H > H_{c2}$ is confirmed by cusplike angular dependence of magnetoresistance. Our data indicates that surface superconductivity is remarkably robust even in disordered polycrystalline films and, surprisingly, even in perpendicular magnetic fields. We conclude that surface superconductivity, rather than flux-flow phenomenon, inhomogeneity, or superconducting fluctuations, is the primary cause of broadening of superconducting transition in magnetic field.

DOI: 10.1103/PhysRevB.94.214506

I. INTRODUCTION

Superconductivity occurs as a result of the second-order phase transition, accompanied by a sudden appearance of the superconducting order parameter below the critical temperature T_c and the upper critical field H_{c2} [1]. This should lead to an abrupt vanishing of resistance. However, in reality resistive transitions are always broadened, especially in a magnetic field. This is usually ascribed to a flux-flow phenomenon caused by motion of Abrikosov vortices [2]. Broadening can also be caused by spatial inhomogeneity (e.g., variation of T_c). In very thin granular films the inhomogeneity can be due to the electronic shell effect [3]. Broadening can be also caused by superconducting fluctuations [4–6], particularly for high temperature superconductors. Finally, surface superconductivity (SSC) may survive up to a significantly higher field $H_{c3} \simeq 1.69H_{c2}$ than bulk superconductivity [1], which can also smear out the superconducting transition at high magnetic fields. Although SSC is quite profound in polished clean superconductors [7–10], it is usually ignored for disordered, polycrystalline films because SSC is considered to be very sensitive to the quality of the surface (e.g., surface passivation [9] and order parameter suppression [1]), surface roughness [7,9], and surface scattering [11].

The presence of several mechanisms of broadening of the superconducting transition makes the interpretation of broadening ambiguous. The lack of understanding does not allow confident extraction of fundamental parameters of superconductors, such as H_{c2}, because it is unclear which point at the transition curve corresponds to $H = H_{c2}$. Arbitrary criteria, such as 10%, 50%, or 90% of the normal state resistance R_n, are commonly applied, which apparently does not work for high-T_c superconductors with very broad transitions [12]. Therefore, clarification of the mechanism of broadening is important both for fundamental and applied research on superconductors.

In this work we study the origin of broadening of superconducting transitions in sputtered Nb films. We perform simultaneous tunneling spectroscopy and transport measurements, which allow unambiguous ascription of H_{c2} to the bottom of resistive transition $R(H_{c2})/R_n \sim 0$. The top of transition corresponds to ~ 1.7 times higher fields, which is close to the third critical field H_{c3} for destruction of surface superconductivity. The two-dimensional (2D) nature of SSC at $H_{c2} < H < H_{c3}$ is confirmed by observation of cusplike angular dependence of magnetoresistance. Thus we conclude that surface superconductivity, rather than flux-flow, inhomogeneity or fluctuations, is the primary cause of broadening of superconducting transitions in magnetic field. Our data indicates that surface superconductivity is remarkably robust even in disordered polycrystalline films and, surprisingly, even in perpendicular magnetic fields. Therefore, surface superconductivity has to be considered for proper analysis of the fluctuation superconductivity.

II. EXPERIMENT

The studied sample contains several Nb/Al-AlO_x/Nb tunnel junctions with sputtered Nb electrodes of thicknesses $d = 150$ and 50 nm. Junction characteristics in perpendicular fields were reported in Ref. [13]. Due to different thicknesses, electrodes have slightly different T_c of 9.2 and 8.8 K. Parameters extracted from tunneling characteristics are determined by the thinner electrode, while transport measurements are made at the thicker electrode. This explains a minor difference in H_{c2} values obtained by those techniques. Measurements are performed in a gas-flow ^{4}He cryostat with a superconducting solenoid. Samples are mounted on a rotatable holder with the alignment accuracy $\sim 0.02^\circ$. Details of the setup can be found elsewhere [13].

III. RESULTS

In Figs. 1(a)–1(c) we show superconducting transitions of a 150 nm thick Nb film: (a) $R(T)$ in zero field and $R(H)$ at $T = 1.8$ K for field perpendicular (b) and parallel (c) to the film. It is seen that at zero field the $R(T)$ transition is very sharp and does not show any extended fluctuation region or inhomogeneity. However, $R(H)$ transitions are quite broad. Interestingly, $R(H)$ is broader when the field is parallel

*Vladimir.Krasnov@fysik.su.se

 ©2016 American Physical Society

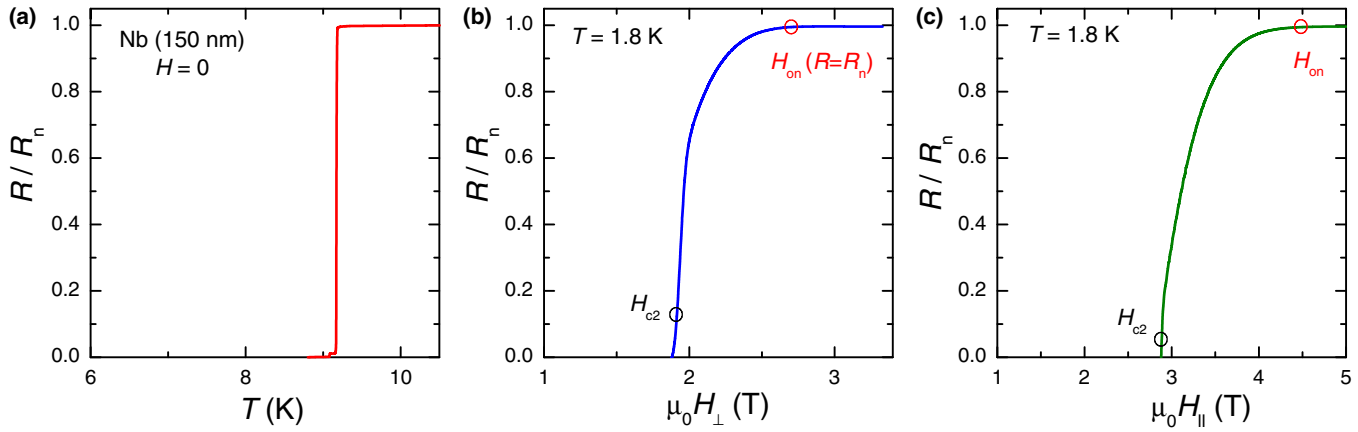

FIG. 1. Resistive transitions of a 150 nm thick Nb film. (a) Temperature dependence of the resistance in zero magnetic field. (b) and (c) Field dependencies of resistances at $T = 1.8$ K in fields (b) perpendicular and (c) parallel to the film. Black and red circles mark the upper critical field H_{c2} and the field of the onset of resistive transition, which coincides with the critical field of surface superconductivity $H_{on} \sim H_{c3}$.

to the film. This confronts interpretation of broadening in terms of vortex motion because the driving Lorentz force is most effective in perpendicular and vanishes in parallel field. Therefore, this broadening is not consistent with either flux-flow, inhomogeneity, or fluctuation mechanisms.

A. Determination of H_{c2} from tunneling spectroscopy

In order to analyze surface superconductivity scenario, first of all, it is necessary to determine bulk H_{c2}. For this we perform magneto-tunneling spectroscopy. Figure 2 represents a comparison of theoretically calculated [panels (a)–(c)]

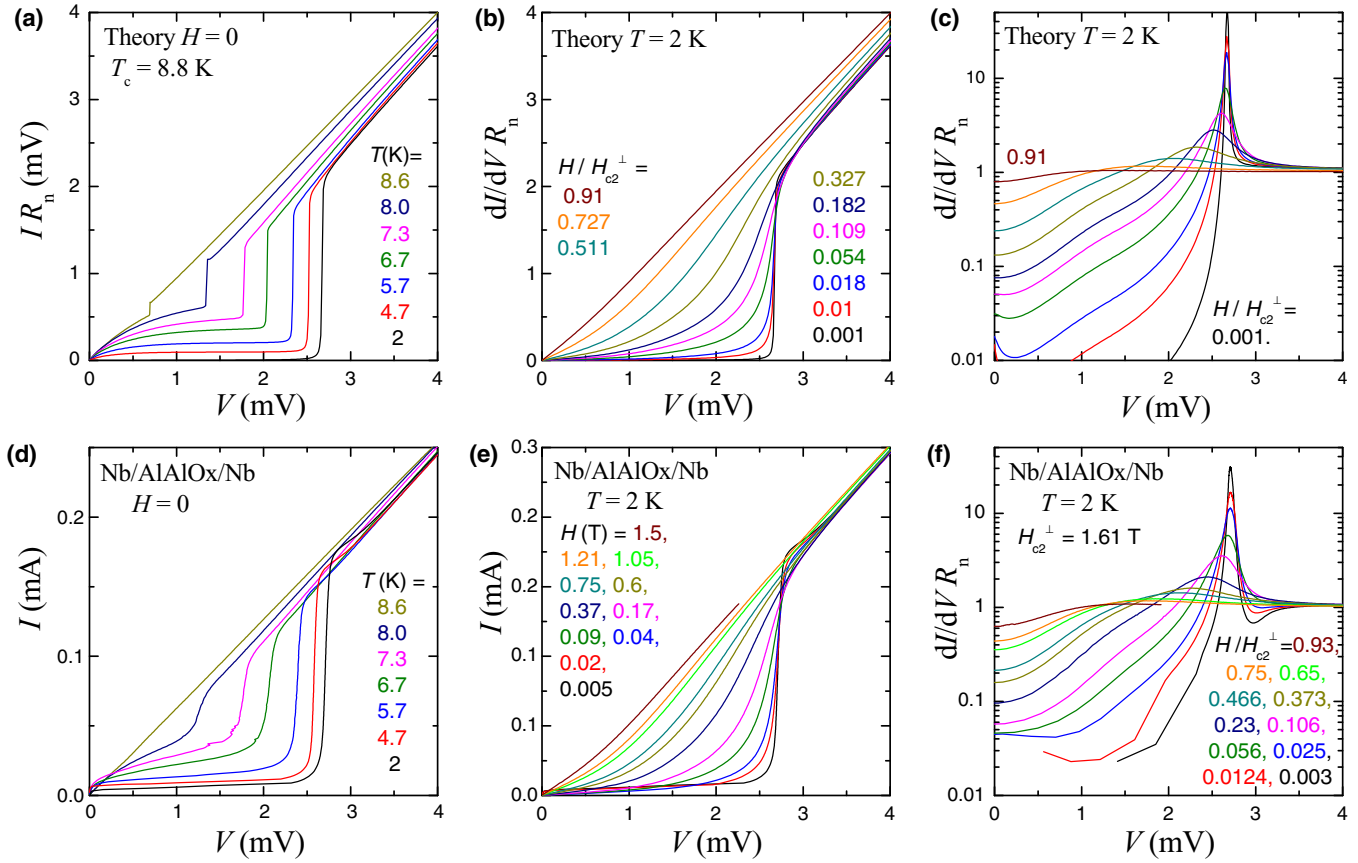

FIG. 2. Comparison of theoretically calculated [(a)–(c)] and experimentally measured [(d)–(f)] characteristics of Nb/Al-AlO$_x$/Nb tunnel junctions. (a) and (d) Temperature dependence of I-V characteristics at zero field. (b) and (e) Field dependence of I-V characteristics for field perpendicular to the junction/films at $T \simeq 2$ K. (c) and (f) The corresponding differential conductances for curves from panels (b) and (e). The field scale in (f) is normalized by the upper critical field $H_{c2}^{\perp} = 1.61$ T, which is obtained as a single scaling factor for all the curves at different fields. Data are from Ref. [13].

and experimentally measured tunneling characteristics of our Nb/Al-AlO$_x$/Nb junction (data from Ref. [13]). Panels (a) and (d) show temperature dependencies of I-V characteristics at zero field. Panels (b) and (e) show field dependence of I-V characteristics for field perpendicular to the junction/films at $T \simeq 2$ K. Panels (c) and (f) show the corresponding differential conductances for I-V curves from panels (b) and (e).

At $H_{c1} < H < H_{c2}$ type-II superconductors are in the mixed state, characterized by the presence of Abrikosov vortices with spatially inhomogeneous order parameter and density of states. Increase of magnetic field leads to increase of the vortex density, i.e., decrease of the unit cell size of the vortex lattice. Theoretical calculations shown in Fig. 2 represent tunneling characteristics averaged over one unit cell of the vortex lattice. Details of calculations are described in Ref. [13].

From Fig. 2 it is seen that there is a good quantitative agreement between theoretical and experimental characteristics. The main spectroscopic features are the sharp sum-gap peak at $V_p = 2\Delta/e$, where Δ is the superconducting gap, and the suppressed quasiparticle current and conductance below the sum-gap voltage. With increasing field the peak is decreasing in height and is moving to lower voltages. Simultaneously the sub-gap conductance is increased. All this is due to suppression of the spatial average superconducting gap with increasing magnetic field due to entrance of Abrikosov vortices. The extent of suppression depends solely on H/H_{c2}. Above H_{c2} the superconducting gap vanishes and the I-V becomes linear (Ohmic). Thus, the ratio H/H_{c2} uniquely determines the shape of tunneling characteristics in magnetic field. Therefore, as discussed in Ref. [13], the ratio H/H_{c2} can be uniquely determined from analysis of the shape of tunneling characteristics. In Fig. 2(f) the field is normalized by thus obtained $H_{c2}^{\perp} = 1.61$ T. We emphasize that this value is obtained as a single fitting parameter for the whole set of $dI/dV(V)$ characteristics at different H. This removes the uncertainty in determination of H_{c2}.

Figure 3(a) shows a set of tunneling $dI/dV(V)$ characteristics of a Nb/AlO$_x$/Nb junction at $T = 1.8$ K in fields parallel to Nb films. From comparison of Figs. 2(c), 2(f) and 3(a), it can be seen that the influence of magnetic field is qualitatively similar both for parallel and perpendicular field orientations. In Ref. [13] it was shown that the peak height and the peak voltage exhibit universal almost T-independent quasilinear scaling as

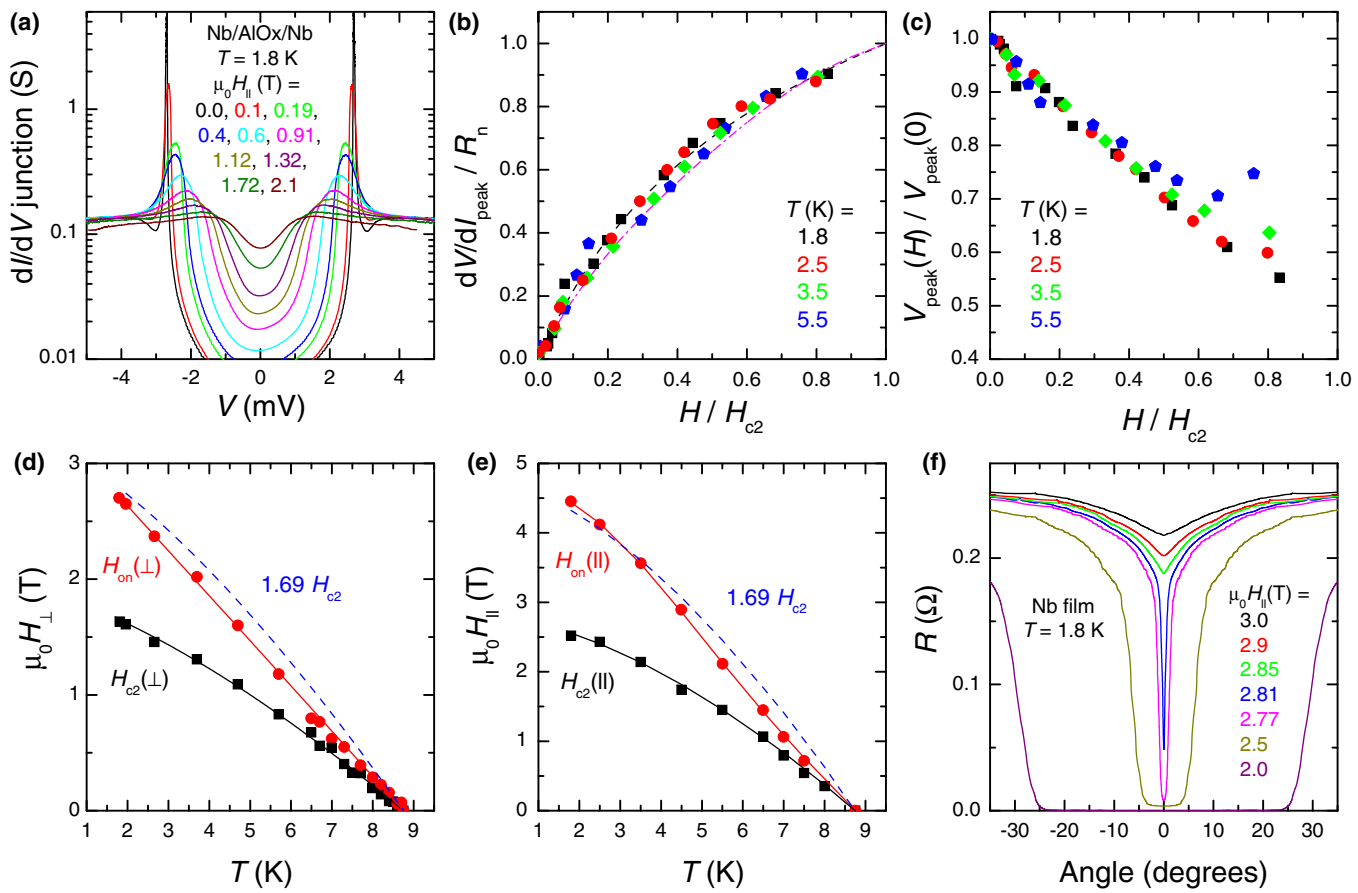

FIG. 3. (a) Differential conductances of a Nb/AlO$_x$/Nb junction (in a semilogarithmic scale) for films parallel to the magnetic fields and $T = 1.8$ K. (b) and (c) Scaling of the sum-gap peak resistance (b) and voltage (c) as a function of $H/H_{c2}(T)$ at different temperatures and parallel fields. Dashed and dashed-dotted lines in (b) represent theoretical curves at $T = 1.96$ and 4.7 K, respectively. (d) and (e) Black squares represent upper critical fields perpendicular (d) and parallel (e) to the films, obtained from the scaling of magneto-tunneling characteristics. Dashed lines represent the expected third critical field for surface superconductivity $H_{c3} = 1.69H_{c2}$. Red circles mark the top onset of the resistive transition. (f) Angular dependence of resistance of Nb electrodes for fields slightly below and above $\mu_0 H_{c2}(\|) = 2.52$ T. A cusplike feature at $H > H_{c2}$ indicates occurrence of the two-dimensional surface superconductivity.

a function of $H/H_{c2}(T)$. Figures 3(b) and 3(c) demonstrate such a scaling at different temperatures for fields parallel to Nb films. Dashed and dashed-dotted lines in Fig. 3(b) represent theoretical results from Ref. [13] for $T = 1.96$ and 4.7 K, respectively. The overall quality of scaling is quite good, which allows confident extraction of $H_{c2}(T)$. Thus obtained H_{c2} is unambiguous because it is deduced as a single fitting parameter for the whole set of $dI/dV(V)$ characteristics at fixed T for different H.

Squares in Figs. 3(d) and 3(e) represent obtained $H_{c2}(T)$ dependencies for perpendicular and parallel field orientations, respectively. Using the relation $H_{c2}^{\perp} = \Phi_0/2\pi\xi^2$ we calculate the coherence length $\xi_0 \simeq 14$ nm. This small value indicates that the film is in the dirty limit with a very short scattering length due to a disordered film structure with nm-scale crystallites. Thus, the studied Nb film $d = 150$ nm is an order of magnitude thicker than ξ_0. This leads to a conclusion, important for a further discussion, that our films are bulk three-dimensional (3D) superconductors practically in the whole temperature range $T < T_c$. Red circles in Figs. 3(d) and 3(e) represent top onsets $R(H_{on}) \simeq R_n$ of resistive transitions, determined as indicated by open circles in Figs. 1(b) and 1(c). Dashed blue lines correspond to $H_{c3} = 1.69H_{c2}$ expected for surface superconductivity, which is close to the onset field. Remarkably this is true even for the perpendicular field orientation when SSC in the uniform case is not expected [1].

B. Angular dependence of magnetoresistance

The 2D nature of SSC should be reflected in a cusplike angular dependence of H_{c3}, given by the equation [14]

$$\left[\frac{H_{c3}(\Theta)}{H_{c3}^{\parallel}}\cos\Theta\right]^2 A(\Theta) + \left|\frac{H_{c3}(\Theta)}{H_{c3}^{\perp}}\sin\Theta\right| = 1, \qquad (1)$$

where $A(\Theta) = 1 + (1 - \sin\Theta)\tan\Theta$. It is only slightly different from Tinkham's 2D result with $A(\Theta) = 1$.

Figure 3(f) shows angular-dependencies of magnetoresistance at $T = 1.8$ K and at different fields below and above $\mu_0 H_{c2}^{\parallel} = 2.52$ T. Zero angle $\Theta = 0$ corresponds to field parallel to the film. At $\mu_0 H = 2.0$ T the film remains in the zero voltage state at small angles because the vortex depinning current is larger than the transport current. At 2.5 T, very slightly below H_{c2}, the film is in the resistive flux-flow state even at $\Theta = 0$ and it is seen that the flux-flow $R(\Theta)$ is flat at $\Theta = 0$, which is characteristic for 3D superconductors such as bulk Nb. However, at $H > H_{c2}^{\parallel}$ angular dependence acquires a 2D cusp. Since the film thickness is much larger than ξ, the observed 2D behavior at low T may originate solely from SSC.

C. Nonlinear bias dependence

The critical surface current density (in A/cm) is [15]

$$I_c \simeq \alpha\frac{H_c}{\kappa}\left(1 - \frac{H}{H_{c3}}\right)^{3/2}. \qquad (2)$$

Here H_c is the thermodynamic critical field (in Oe), κ is the Ginzburg-Landau parameter, and a prefactor $\alpha < 0.1$ [16] is further reduced by surface imperfections. For our films with $\kappa \gg 1$ and width of a few microns the I_c is in the μA range, comparable to the probe current. Therefore, the results do depend on the bias, as illustrated in Fig. 4(a). This is due to strong nonlinearity of current-voltage characteristics at $I \sim I_c$, as demonstrated in Fig. 4(b). In order to demonstrate how such nonlinearity affects experimental characteristics, we consider a standard shape of I-V:

$$V = R_n\sqrt{I^2 - I_c^2}. \qquad (3)$$

Substituting I_c in this equation from Eq. (2) and taking angular dependent H_{c3} from Eq. (1), we obtain for the angular dependence of measured dc resistance

$$1 - \left[\frac{R(\Theta)}{R_n}\right]^2 = \frac{I_c^2}{I^2}\left[1 - \frac{H}{H_{c3}(\Theta)}\right]^{\nu}. \qquad (4)$$

The exponent ν depends on the shape of the I-V curve and the quality of the surface [7]. For the case of Eq. (3) it is $\nu = 3$.

In Fig. 4(c) we show $R(\Theta)$ curves for the SSC model calculated from Eqs. (1) and (4) for $H = 1.1H_{c2}$ at different

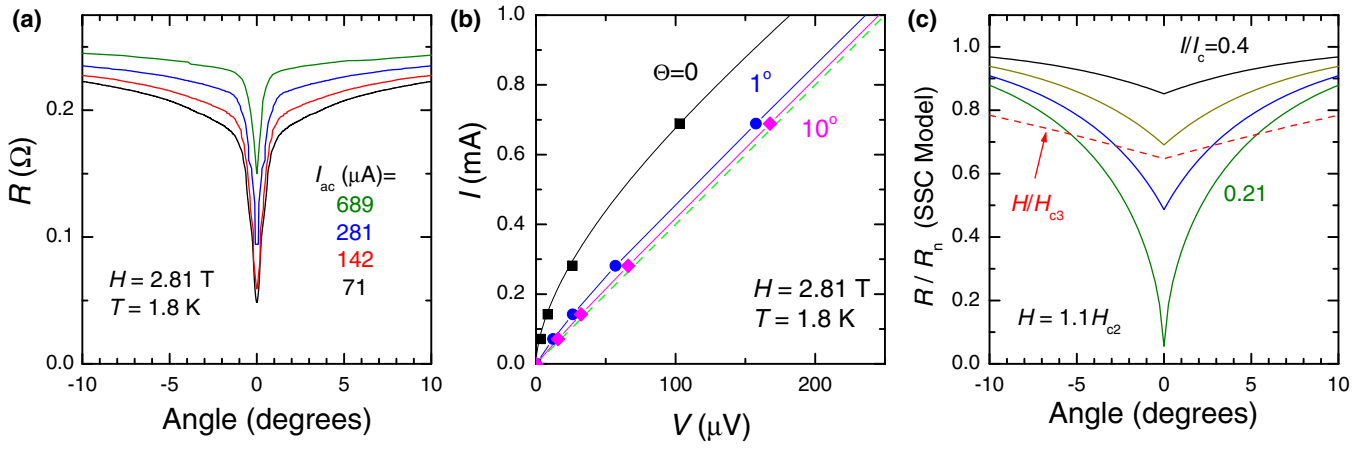

FIG. 4. (a) Bias dependence of $R(\Theta)$ at $T = 1.8$ K and $H = 2.81$ T. (b) Deduced current-voltage characteristics at different angles from the data in panel (a). Dashed line represents the normal state I-V. (c) Simulated angular dependence of $R(\Theta)$ in the surface superconductivity model, taking into account nonlinearity of I-V characteristics in the vicinity of critical current. Solid lines represent calculated of $R(\Theta)$ at different bias. The dashed curve represents the standard flux-flow dependence H/H_{c3}.

bias. Calculations are made for $I_c(\Theta) = \text{const}$ and for $H_{c3}^{\perp} = H_{c2}$ and $H_{c3}^{\parallel} = 1.69H_{c2}$ [17]. For comparison we also show flux-flow type dependence $R/R_n = H/H_{c3}$. It is seen that the cusp in the SSC model is much sharper, primarily due to non-linearity of the I-V. Overall behavior is similar to experimental data from Fig. 4(a), even though in experiment a very sharp cusp at $\Theta = 0$ survives up to much higher current. The difference is due to an oversimplified assumption of angular-independent $I_c(\Theta) = \text{const}$, used in calculations. In reality $I_c(\Theta)$ may have a strong angular dependence at $\Theta = 0$ due to a large aspect ratio (width-to-thickness) of our films. It is possible to get a better fit using a more realistic $I_c(\Theta)$, but we don't want to go in to more complicated modeling because the main purpose of calculations was to demonstrate how non-linearity of I-V's leads to a much sharper (compared to a simple 2D flux-flow model) cusp in $R(\Theta)$.

D. Analysis of fluctuation contribution

Finally we discuss fluctuation contribution to the broadening of resistive transition. In Fig. 5(a) we show normalized excess conductance $\Delta S = (1/R - 1/R_n)R_n$ for the data from Figs. 1(b) and 1(c) in a double-logarithmic scale. Such a graph is usually used for analysis of fluctuation contribution to conductivity. The dashed line shows $\Delta S \propto (H - H_{c2})^{-1}$ dependence expected for 2D fluctuations [4]. It is seen that, although there is a narrow range of fields close to H_{c2} with similar behavior, the overall agreement is poor. In Fig. 5(b) we replot the same data in a semilogarithmic scale. It is seen that ΔS decays quasi-exponentially with increasing field at approximately the same rate for both field orientations. A similar exponential decay versus both T and H has been reported for high-T_c cuprates [13,18–20]. Here we demonstrate that it is generic also for conventional superconductors. Such behavior is not expected for fluctuations [4–6] and we argue that it is rather a signature of SSC.

It is possible to distinguish fluctuation contribution from nonfluctuating SSC. SSC always leads to excess conductance, but fluctuation contribution to magnetoresistance can be both positive and negative [4–6]. In particular, at low T and for field perpendicular to the film, the density-of-state contribution to fluctuations leads to excess resistance, rather than excess conductance [5]. We clearly see such a contribution in our data. In Fig. 5(c) we show high-field part of excess conductance in linear scale. It is seen that in parallel field there is always an excess conductance $\Delta S > 0$, which rapidly decreases upon approaching the surface critical field $H_{c3} \simeq 1.7H_{c2}^{\parallel}$, but never really vanishes. The remaining tail is a signature of fluctuations that persist at any field. For perpendicular field, ΔS at high fields becomes *negative*, which is consistent with theoretical expectations for fluctuation contribution at $T \ll T_c$ [5].

In Fig. 5(d) we check the power-law scaling suggested by Eq. (4) for SSC. It is seen that there is a good scaling in a broad field range, although extraction of the exponent ν is not very confident because it depends on the chose of H_{c3}. The dashed line corresponds to $\nu = 4.8$. Upon approaching H_{c3},

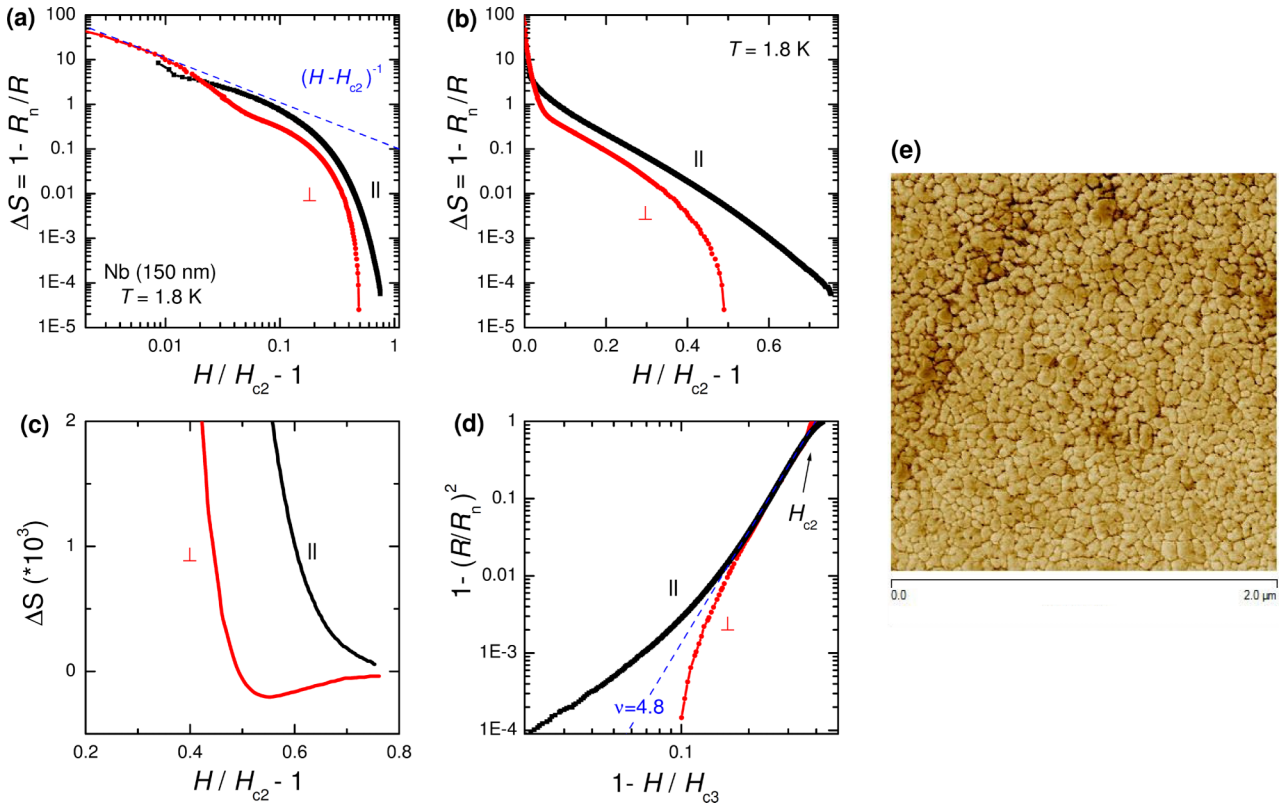

FIG. 5. (a) and (b) Excess conductance vs magnetic field at $T = 1.8$ K plotted in (a) a double-logarithmic and (b) a semilogarithmic scale. Quasi-exponential decay $\Delta S(H)$ is seen. (c) The high-field part of excess conductance. It reveals a fluctuation contribution, which is positive for parallel but negative for perpendicular field orientation. (d) Analysis of power-law scaling expected for surface superconductivity according to Eq. (4). The dashed line represents a power law with the exponent $\nu = 4.8$. (e) AFM image of the studied Nb film.

deviations with opposite signs for parallel and perpendicular field orientations appear, signalizing fluctuation contributions. This indicates that SSC makes a dominant contribution to excess conductivity at $H_{c2} < H \lesssim 0.8H_{c3}$, while fluctuation contribution starts to become significant only upon weakening of SSC at $H > 0.8H_{c3}$ and takes over completely at $H > H_{c3}$.

IV. DISCUSSION

Our results suggest that surface superconductivity is the primary cause of broadening of superconducting transition in magnetic field. As indicated in Figs. 1(b) and 1(c), $H = H_{c2}$ corresponds to the bottom of transition, consistent with earlier studies [21], and H_{c3} to the top of the resistive transition. Thus the full width of the transition is dominated by SSC. Although SSC is well known for carefully polished single crystals [8,10], it is usually considered to be insignificant for disordered, rough or inhomogeneous superconducting films because of its assumed fragility and sensitivity to surface conditions [1,7,9,11]. Therefore, observation of a very robust SSC in our strongly disordered polycrystalline films is rather surprising, especially for field perpendicular to the film. In perfectly uniform films SSC should not occur at perpendicular field orientation [1,15]. Yet, SSC in perpendicular fields has been directly visualized by scanning laser microscopy for similar films [22] and also reported for some layered supercondcutors [23] and sintered polycrystalline MgB_2 samples [24].

Fig. 5(e) shows a phase-contrast Atomic-Force microscopy (AFM) image of the studied Nb film surface 2×2 μm^2. It is seen that the film has a columnar structure with columns perpendicular to the substrate and the characteristic column diameter of few tens of nm. This is typical for sputtered Nb films. Presumably it is the polycrystallinity of our films that allows SSC at grain boundaries even in perpendicular fields. This is consistent with previous reports about "internal surface" superconductivity at grain boundaries in severely deformed Nb [25,26].

Thus we conclude that surface superconductivity is a robust phenomenon that should be carefully considered in analysis of data close to the superconducting transition. In particular, we have shown that surface superconductivity, rather than flux-flow phenomenon, inhomogeneity, or fluctuations, is the primary cause of broadening of the superconducting transition in the studied films at high magnetic fields for both parallel and perpendicular to the film orientations. The upper critical field always corresponded to the bottom of the resistive transition $R(H_{c2}) \sim 0$, while the excess conductance is dominated by non-fluctuating surface superconductivity up to the third critical field $H_{c3} \sim 1.7H_{c2}$, which also corresponds to the top of transition $R(H_{c3}) \simeq R_n$. The fluctuation contribution becomes significant only close and above H_{c3}. Thus our data indicates that it is impossible to correctly analyze the fluctuation contribution without proper consideration of surface superconductivity.

ACKNOWLEDGMENTS

The work was supported by the Swedish Research Council Grant No. 621-2014-4314 and the Swedish Foundation for International Cooperation in Research and Higher Education Grant No. IG2013-5453.

[1] D. Saint-James, G. Sarma, and E. J. Thomas, *Type-II Superconductivity* (Pergamon, Oxford, 1969).

[2] J. Bardeen and M. J. Stephen, Theory of the motion of vortices in superconductors, Phys. Rev. **140**, A1197 (1965).

[3] S. Bose, A. M. García-García, M. M. Ugeda, J. D. Urbina, C. H. Michaelis, I. Brihuega, and K. Kern, Observation of shell effects in superconducting nanoparticles of Sn, Nat. Mater. **9**, 550 (2010).

[4] A. I. Larkin and A. A. Varlamov, *Theory of Fluctuations in Superconductors* (Oxford University Press, New York, 2009).

[5] A. Glatz, A. A. Varlamov, and V. M. Vinokur, Fluctuation spectroscopy of disordered two-dimensional superconductors, Phys. Rev. B **84**, 104510 (2011).

[6] K. S. Tikhonov, G. Schwiete, and A. M. Finkel'stein, Fluctuation conductivity in disordered superconducting films, Phys. Rev. B **85**, 174527 (2012).

[7] R. V. Bellau, Influence of surface condition on the critical currents above H_{c2} in a superconducting tantalum-niobium alloy, Phys. Lett. **21**, 13 (1966).

[8] S. R. Park, S. M. Choi, D. C. Dender, J. W. Lynn, and X. S. Ling, Fate of the Peak Effect in a Type-II Superconductor: Multicriticality in the Bragg-Glass Transition, Phys. Rev. Lett. **91**, 167003 (2003).

[9] S. Casalbuoni, E. A. Knabbe, J. Kötzler, L. Lilje, L. von Sawilski, P. Schmüser, and B. Steffen, Surface superconductivity in niobium for superconducting RF cavities, Nucl. Instrum. Methods Phys. Res., Sect. A **538**, 45 (2005).

[10] P. Das, C. V. Tomy, S. S. Banerjee, H. Takeya, S. Ramakrishnan, and A. K. Grover, Surface superconductivity, positive field cooled magnetization, and peak-effect phenomenon observed in a spherical single crystal of niobium, Phys. Rev. B **78**, 214504 (2008).

[11] D. F. Agterberg and M. B. Walker, Effect of diffusive boundaries on surface superconductivity in unconventional superconductors, Phys. Rev. B **53**, 15201 (1996).

[12] A. S. Alexandrov, V. N. Zavaritsky, W. Y. Liang, and P. L. Nevsky, Resistive Upper Critical Field of High-T_c Single Crystals of $Bi_2Sr_2CaCu_2O_8$, Phys. Rev. Lett. **76**, 983 (1996).

[13] V. M. Krasnov, H. Motzkau, T. Golod, A. Rydh, S. O. Katterwe and A. B. Kulakov, Comparative analysis of tunneling magnetoresistance in low-T_c Nb/Al-AlO_x/Nb and high-T_c $Bi_{2-y}Pb_ySr_2CaCu_2O_{8+d}$ intrinsic Josephson junctions, Phys. Rev. B **84**, 054516 (2011).

[14] K. Yamafuji, E. Kusayanagi, and F. Irie, On the angular dependence of the surface superconducting critical field, Phys. Lett. **21**, 11 (1966).

[15] A. A. Abrikosov, Concerning surface superconductivity in strong magnetic fields, Sov. Phys. JETP **20**, 480 (1965).

[16] J. G. Park, Asymmetry in the Critical Surface Current of Type-2 Superconductors, Phys. Rev. Lett. **15**, 352 (1965).

[17] For modeling in Fig. 4(c) we assumed $H_{c3}^{\parallel}/H_{c3}^{\perp} = 1.69$, which is roughly equal to the anisotropy of the upper critical field; see Figs. 3(d) and 3(e). The latter in turn is due to flatness of the film with the thickness comparable to London penetration depth.

[18] S. O. Katterwe, Th. Jacobs, A. Maljuk, and V. M. Krasnov, Low anisotropy of the upper critical field in a strongly anisotropic layered cuprate $Bi_{2.15}Sr_{1.9}CuO_{6+\delta}$: Evidence for a paramagnetically limited superconductivity, Phys. Rev. B **89**, 214516 (2014).

[19] F. Rullier-Albenque, H. Alloul, and G. Rikken, High-field studies of superconducting fluctuations in high-T_c cuprates: Evidence for a small gap distinct from the large pseudogap, Phys. Rev. B **84**, 014522 (2011).

[20] H. Luo and H. H. Wen, Localization of charge carriers in the normal state of underdoped $Bi_{2+x}Sr_{2-x}CuO_{6+\delta}$, Phys. Rev. B **89**, 024506 (2014).

[21] J. P. Burger, G. Deutscher, E. Guyon, and A. Martinet, Behavior of first- and second-kind superconducting films near their critical fields, Phys. Rev. **137**, A853 (1965).

[22] R. Werner, A. Yu. Aladyshkin, I. M. Nefedov, A. V. Putilov, M. Kemmler, D. Bothner, A. Loerincz, K. Ilin, M. Siegel, R. Kleiner and D. Koelle, Edge superconductivity in Nb thin film microbridges revealed by electric transport measurements and visualized by scanning laser microscopy, Supercond. Sci. Technol. **26**, 095011 (2013).

[23] F. Levy-Bertrand, B. Michon, J. Marcus, C. Marcenat, J. Kačmarčik, T. Klein, and H. Cercellier, Puzzling evidence for surface superconductivity in the layered dichalcogenide $Cu_{10\%}TiSe_2$, Physica C **523**, 19 (2016).

[24] M. I. Tsindlekht, G. I. Leviev, V. M. Genkin, I. Felner, P. Mikheenko, and J. S. Abell, Surface superconducting states in a polycrystalline MgB_2 sample, Phys. Rev. B **74**, 132506 (2006).

[25] S. J. Williamson and J. K. Furdyna, Orientation dependence of the resistive transition near H_{c2} in high field superconductors, Phys. Lett. **21**, 376 (1966).

[26] D. C. Hill, J. G. Kohr, and R. M. Rose, Evidence for "internal surface" superconductivity in severely deformed niobium, Phys. Lett. A **31**, 157 (1970).